BASIC SCIENCE

Nanomedicine: Nanotechnology, Biology, and Medicine
30 (2020) 102285

nanomedicine
Nanotechnology, Biology, and Medicine

Original Article

nanomedjournal.com

Exosome mediated delivery of functional nucleic acid nanoparticles (NANPs)

Senny Nordmeier, PhD[a,1], Weina Ke, BS[b,1], Kirill A. Afonin, PhD[b,*], Victoria Portnoy, PhD[a,*]

[a]*System Biosciences (SBI), Palo Alto, CA, USA*
[b]*Nanoscale Science Program, Department of Chemistry, University of North Carolina at Charlotte, Charlotte, NC, USA*

Revised 25 July 2020

Abstract

RNAi-based technologies have shown biomedical potential; however, safe and efficient delivery of RNA remains a barrier for their broader clinical applications. Nucleic acid nanoparticles (NANPs) programmed to self-assemble and organize multiple therapeutic nucleic acids (TNAs) also became attractive candidates for diverse therapeutic options. Various synthetic nanocarriers are used to deliver TNAs and NANPs, but their clinical translation is limited due to immunotoxicity. Exosomes are cell-derived nanovesicles involved in cellular communication. Due to their ability to deliver biomolecules, exosomes are a novel delivery choice. In this study, we explored the exosome-mediated delivery of NANPs designed to target GFP. We assessed the intracellular uptake, gene silencing efficiency, and immunostimulation of exosomes loaded with NANPs. We also confirmed that interdependent RNA/DNA fibers upon recognition of each other after delivery, can conditionally activate NF-kB decoys and prevent pro-inflammatory cytokines. Our study overcomes challenges in TNA delivery and demonstrates future studies in drug delivery systems.

Key words: Extracellular vesicles; Exosomes; RNA nanotechnology; NANPs; Immunostimulation

Nucleic acid nanoparticles (NANPs) are modular nanoscaffolds exclusively made of multiple oligonucleotides programmed to self-assemble into precise 3D structures with well-defined properties.[1–4] Rationally designed NANPs can be further decorated with cocktails of therapeutic nucleic acids (TNAs), which may differ in composition, secondary structure, and mechanism of action, allowing for synchronized targeting of multiple cellular pathways. This structural versatility – and ability to finely control the NANPs' sizes, shapes, composition, multivalences, and therapeutic payloads – makes this technology an attractive option for biomedical applications.[5–7] For example, a previously tested combinatorial RNAi strategy of NANPs functionalized with six different Dicer substrate (DS) RNAs[8] were effective in simultaneous targeting six distinct parts of the HIV-1 genome.[1,9] These NANPs functionalized with DS RNAs relied on the assistance from the intracellular enzyme Dicer that initiated the nuclease-assisted release of siRNAs from the NANPs. Moreover, by simply extending either the 5′- or/and 3′- ends of each strand of the NANP's composition with its unique functionality, NANPs can be formulated to precisely package not only different TNAs but also fluorophores, targeting agents, small-molecule drugs, proteins, or other therapeutic cargoes.[10–12]

A sophisticated approach to the conditional intracellular activation of RNAi was introduced through interdependent RNA/DNA NANPs in which the RNA (and/or DNA) functionalities were split into two inactive NANPs.[13–15] Driven by sequence complementarity, the inactive NANPs could recognize each other inside the cells and release the activated functionalities upon isothermal reassociation.[2,9,16] Using the same approach, RNA/DNA fibers were recently designed for enhanced control of deliverable functionalities (*e.g.,* DS RNAs targeting mutated $BRAF^{V600E}$ in melanoma cells) along with higher stability against enzymatic degradation in human blood and tunable rates of intracellular reassociation.[17] Another advantage of this user-friendly approach: the DNA part of the

Conflict of interests

*Corresponding authors.
E-mail addresses: kafonin@uncc.edu, (K.A. Afonin), vportnoy@systembio.com. (V. Portnoy).
[1] Equal contribution

https://doi.org/10.1016/j.nano.2020.102285

Please cite this article as: Nordmeier S, et al, Exosome mediated delivery of functional nucleic acid nanoparticles (NANPs). *Nanomedicine: NBM* 2020;30:102285, https://doi.org/10.1016/j.nano.2020.102285

RNA/DNA fibers contained split NF-kB (nuclear factor kappa-light-chain enhancer of activated B cells) decoy sequences, which activate upon intracellular fiber reassociation and restrain the immunostimulatory response. NF-kB is expressed in most mammalian cells and remains sequestered in an inactive state in the cytoplasm with the inhibitory protein IκB. Activation of NF-kB is initiated by a variety of stimuli, resulting in signal-induced degradation of IκB proteins by proteasomes. Subsequently, the NF-κB complex can enter the nucleus and initiate gene expression of pro-inflammatory cytokines. NF-κB decoys[18–20] mimic the κB consensus sequence and upon the decoy's binding to NF-κB its nuclear translocation becomes attenuated.

Since all NANPs are composed of negatively charged, hydrophilic biopolymers, they cannot easily penetrate through the hydrophobic biological membranes and thus, mainly rely on the use of different synthetic carriers for efficient intracellular delivery.[17,21–25] Over the last few decades, extensive research efforts have been undertaken to improve the stability, efficacy, and specificity of TNA delivery systems, such as liposomes,[26] micelles,[27] nanoparticles,[28] hydrogels,[29] and viruses.[30] In spite of these massive attempts, most of these systems suffer from immunogenicity, cytotoxicity, rapid blood clearance, and poor biodistribution,[31] hindering further clinical translation of therapeutic NANP platforms. Therefore, an urgent need to identify new endogenous sources for potential delivery systems that avoid the complications associated with synthetic materials is vital.

Extracellular vehicles (EVs) are membrane enclosed vesicles ranging from 30 nm to 1000 nm (or even larger) in size and secreted by cells into the extracellular space.[32,33] EVs comprise of exosomes and microvesicles, which are differentiated by their biogenesis, content, size, release pathways, and function.[34] Exosomes have been widely investigated as emerging novel delivery vehicles for biological cargos. These structures range from 30 nm to 150 nm in size[35] and are released into most biological fluids. Biological molecules, such as proteins, lipids, and nucleic acids, undergo transport *via* exosomes from the cell of origin to recipient cells.[36] Exosomes form by inward budding of the cell membrane, a process which generates early endosomes. After the endosomes mature into multivesicular bodies (MVB), they fuse with the cell membrane and exit from the cell; alternatively, they can fuse with a lysosome for degradation. (Figure 1, *A*).[37] Reflective of the mechanism of biogenesis, exosomes are considered to be the "mini versions" of their parental cells in terms of the specially sorted "cargo" they carry.[38] The putative function of exosomes is to perform intercellular communication and trigger physiological responses. Interaction between exosomes and recipient cells is promoted *via* receptor-mediated endocytosis,[39] micropinocytosis,[40] or membrane fusion.[41] Once internalized, the exosomal contents are released into the cytosol directly or through back-fusion with the endosomal membrane, eliciting the effect on the recipient cell.[42] Such features of the exosomes highlight their potential as drug delivery systems to alter gene expression by delivering therapeutic genetic materials. Several studies have investigated their performance as therapeutic vehicles for exogenous genetic material delivery as well as their post-delivery functionality. The first published study showed that exosomes could efficiently deliver exogenous siRNAs to the brains of mice with successful knockdown of mRNA and BACE1 protein with negligible immune response.[43] Later, a myriad of studies reported using exosomes to deliver siRNAs and knockdown targeted genes in different diseases. For example, exosome-mediated delivery has shown promise in silencing specific genes, including VEGF, EGFR, AKT, MAPK, and KRAS[44]; inhibiting luciferase expression[45]; treating hepatitis C infection; causing massive cell death of recipient cells by RAD51 gene suppression[46]; and survivin siRNA suppression for the treatment of bladder cancer.[47] Recently, exosomes derived from normal fibroblast-like mesenchymal cells were engineered to carry shRNAs or siRNAs against the KrasG12D mutation known for triggering pancreatic cancer growth in multiple mouse models.[48] The use of exosomes as delivery vehicles demonstrates a plethora of advantages, including biocompatibility, efficacy, stability, and membrane permeation capability; as well as diminished toxicity; low immunogenicity; low off-target effect; and the ability to cross the blood–brain-barrier.[31,49–53] As a result, exosomes can significantly outperform other delivery methods.

In this work, we investigated the use of exosomes as carriers for delivering functional NANPs of different shapes, sizes, and compositions, among which were globular RNA cubes, planar RNA rings, and linear RNA/DNA fibers. We assessed, *in vitro*, the stability of exosome-loaded NANPs, in addition to their intracellular uptake, silencing efficiency, and immunostimulatory activity.

Methods

All experimental details and sequences used in this work are listed in the Supplementary Material.

Cell culture

MDA-MB-231-GFP, MDA-MB-231 and HUVEC cells were used in this study. All oligonucleotides were purchased from Integrated DNA Technologies (IDTDNA.com, Coralville, IA, USA). All NANP compositions used in this project are listed in the Supplementary Material Table 1.

Assemblies of RNA/DNA fibers, RNA cubes and RNA rings targeting GFP and their analysis by native-PAGE

All individual strands were purified by an 8 M urea polyacrylamide gel (8% acrylamide, 19:1), gel extracted, eluted and dissolved in endotoxin-free water. All individual RNA strands for cube and rings were synthesized *via in vitro* run-off transcription (IVT) assay, purified by an 8 M urea polyacrylamide gel (8% acrylamide, 19:1), gel extracted, eluted and dissolved in endotoxin-free water. RNA/DNA fibers, RNA cubes, and RNA rings were assembled in one-pot by combining individual monomers at equimolar concentrations in an assembly buffer. All NANPs were analyzed on 8% non-denaturing native polyacrylamide gel (19:1 for fibers, 37.5:1 for rings and cubes).

Atomic force microscopy (AFM) imaging of NANP

A freshly cleaved mica surface modified with APS (1-(3-aminopropyl) silatrane) was used for AFM imaging, which was performed on the MultiMode AFM NanoScope IV system (Bruker Instruments, Santa Barbara, CA, USA) in tapping mode.

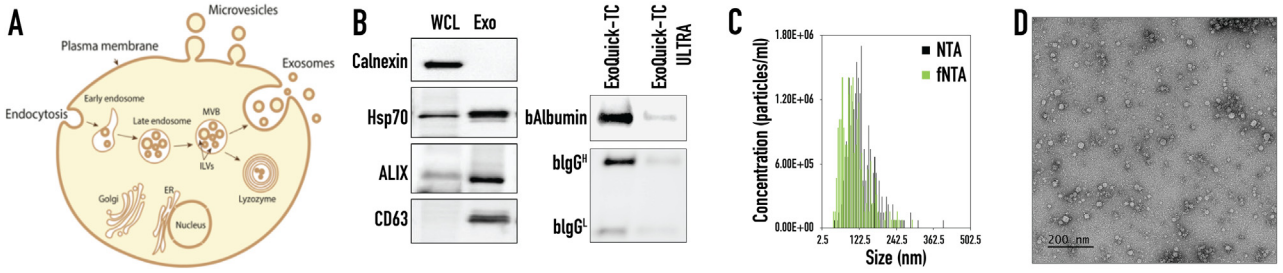

Figure 1. Characterization of exosomes isolated from MDA-MB-231 cells**.** (**A**) Schematic representation of exosome formation and release out to the extracellular space. (**B**) Western blot analysis of exosomal markers for CD63, ALIX and Hsp70, and cellular ER marker Calnexin in the whole cell lysate (WCL) and ExoQuick-TC ULTRA isolated exosomes (Exo). Western Blot analysis of the co-isolating proteins, bovine albumin (bAlbumin) and bovine immunoglobulin (bIgG) after one isolation step of precipitation step with ExoQuick-TC and after two steps of precipitation with ExoQuick-TC ULTRA. (**C**) The size distribution of isolated exosomes showing concentration in particles/mL. (**D**) TEM analysis of isolated exosomes.

Nuclease protection assay of DNA duplex

125 nM dsDNA labeled with Alexa Fluor 488 at the 5′ sense strand and an Iowa Black Quencher at the 3′ antisense strand was loaded into exosomes and then treated with RQ1 DNase I. The fluorescence resulting from the digestion of the DNA duplex by RQ1 DNase was monitored at 37 °C for a total of 60 min with measurements at every 30 s. Free fluorescently quenched DNA duplex was used as the control.

Isolation of exosomes

Exosomes were isolated from MDA-MB-231 or HUVEC cells using ExoQuick-TC ULTRA (System Biosciences, Palo Alto, CA, USA) according to the manufacturer's manual. Protein concentration was measured by Qubit protein assay and all exosomes were stored at −20 °C.

Immunoblotting

5 μg of isolated exosomes was run on 4%-20% Mini-PROTEAN TGX gel, transferred to PVDF membrane and probed with primary antibodies overnight. Next day, the membranes were washed three times, probed with appropriate secondary antibody and imaged using Molecular Imager ChemiDOC XRS+ Imaging System (Bio-Rad, Hercules, CA, USA).

Nanoparticle tracking analysis and exosomes labeling for f-NTA

Isolated exosomes were labeled with the ExoGlow-NTA fluorescent kit (System Biosciences, Palo Alto, CA, USA). Labeled exosomes were stored at −20 °C until the analysis. Unlabeled and labeled samples were analyzed by NTA and f-NTA using ZetaView.

TEM analysis

Isolated exosomes were fixed by addition of 4% paraformaldehyde; 5 μl of the sample was dropped on a carbon coated 400 mesh Cu/Rh grid (Ted Pella, Redding, CA, USA) and stained with 5 μl of 1% uranyl acetate (Polysciences, Warrington, PA, USA) prepared in filtered distilled water. The grids were imaged with an FEI Talos L120C TEM with Gatan 4 k × 4 k OneView camera.

Loading of exosomes with NANPs

100 μg of isolated exosomes was loaded with 25 pmol NANPs using the Exo-Fect siRNA/miRNA transfection kit (System Biosciences, Palo Alto, CA, USA) according to the manufacturer's manual. The loaded exosomes were cleaned to remove any excess of free NANPs/negative control siRNA, transfection reagent, or complexes. The cleaned NANP loaded exosomes were immediately added onto MDA-MB-231-GFP cells.

RNA purification and quantitative real time PCR (RT-qPCR) analysis

Total RNA was purified using RNeasy Plus Mini kit (Qiagen, Hilden, Germany) according to the manufacturer's manual. Purified total RNA was reverse transcribed using anchor Oligo $(dT)_{20}$ primer (Thermo Fisher Scientific, Wilmington, DE, USA) and Superscript III reverse transcriptase (Thermo Fisher Scientific, Wilmington, DE, USA). Real time qPCR was performed using TaqMan Fast Advanced Master Mix (Thermo Fisher Scientific, Wilmington, DE, USA) with TaqMan gene expression assay eGFP (Thermo Fisher Scientific, Wilmington, DE, USA, Mr04097229_mr) and with TaqMan gene expression assay Beta-2-microglobulin as a reference gene (Thermo Fisher Scientific, Hs00984230_m1, Wilmington, DE, USA) and the QuantStudio 6 FLEX (Applied Biosystems, Thermo Fisher Scientific, Wilmington, DE, USA).

Flow cytometry

MDA-MB-231-GFP treated cells were trypsinized with 0.25% trypsin–EDTA (Thermo Fisher Scientific, Waltham, MA, USA) for 2 min at 37 °C, quenched with DMEM supplemented with 10% FBS, and pelleted by centrifugation at 800 ×*g* for 2 min. The cell pellet was resuspended with 1× PBS supplemented with 1% FBS into a 12 × 75 mm test tube with a cell strainer cap (Falcon, Durham, NC, USA) and analyzed with the DxP FACScan (Cytek Biosciences, Fremont, CA, USA). The data were analyzed using FCS Express 5 (De Novo Software, Glendale, CA, USA).

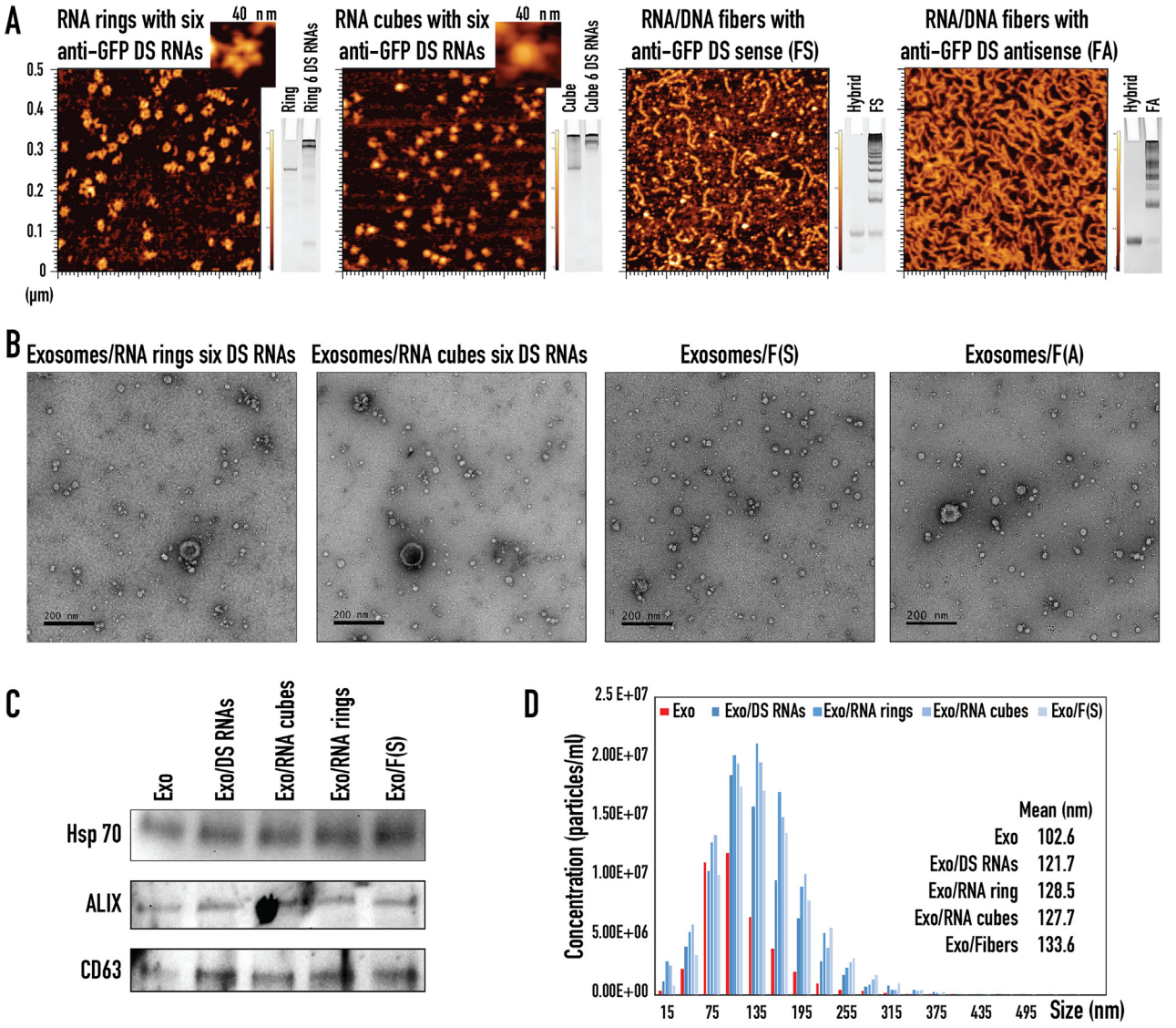

Figure 2. Characterization of various functionalized NANPs and NANP loaded exosomes. (**A**) Representative AFM images and native-PAGE results of RNA rings with six anti-GFP Dicer substrate (DS) RNAs, RNA cubes with six anti-GFP DS RNAs, RNA/DNA fibers with anti-GFP DS sense, and RNA/DNA fibers with anti-GFP DS antisense. (**B**) TEM images of exosomes loaded with RNA rings with six anti-GFP DS RNAs, RNA cubes with six anti-GFP DS RNAs, RNA/DNA fibers with anti-GFP DS sense, and RNA/DNA fibers with anti-GFP DS antisense. (**C**) Western blot analysis of exosomal markers for CD63, ALIX, and Hsp70 in ExoQuick-TC ULTRA isolated exosomes (Exo) taken through the loading steps as negative control and exosomes loaded with anti-GFP DS RNAs (Exo/DS RNAs), RNA cubes with six anti-GFP DS RNAs (Exo/RNA cubes), RNA rings with six anti-GFP DS RNAs (Exo/RNA rings), and RNA/DNA fibers with anti-GFP DS sense (Exo/Fibers). (**D**) NTA analysis of ExoQuick-TC ULTRA isolated exosomes (Exo) taken through the loading steps as negative control and exosomes loaded with anti-GFP DS RNAs (Exo/DS RNAs), RNA cubes with six anti-GFP DS RNAs (Exo/RNA cubes), RNA rings with six anti-GFP DS RNAs (Exo/RNA rings), and RNA/DNA fibers with anti-GFP DS sense (Exo/Fibers).

Cell uptake imaging

Cells transfected with NANP loaded exosomes or negative control loaded exosomes were imaged 72 h post-transfection. For the cancer and primary cells transfected with exosomes loaded with DNA cube-Alexa 488, cells were imaged 24 h post-transfection. The images were captured using a Leica DMI3000 inverted microscope with a DFC360 FX digital camera (Leica Microsystems, Wetzlar, Germany).

Immunostimulation in vitro

HEK-Blue™ hTLR3 and 7 cells, and THP1-Dual™ cells (Invivogen, San Diego, CA, USA) were used for quantifying the activation of specific toll-like receptor (TLR) and intracellular signaling pathways, respectively. HEK-Blue™ hTLR 3 and 7 cells are HEK cells engineered to stably co-express human TLR and NF-κB-inducible SEAP (secreted embryonic alkaline phosphatase) reporter genes. The TLR activation results in

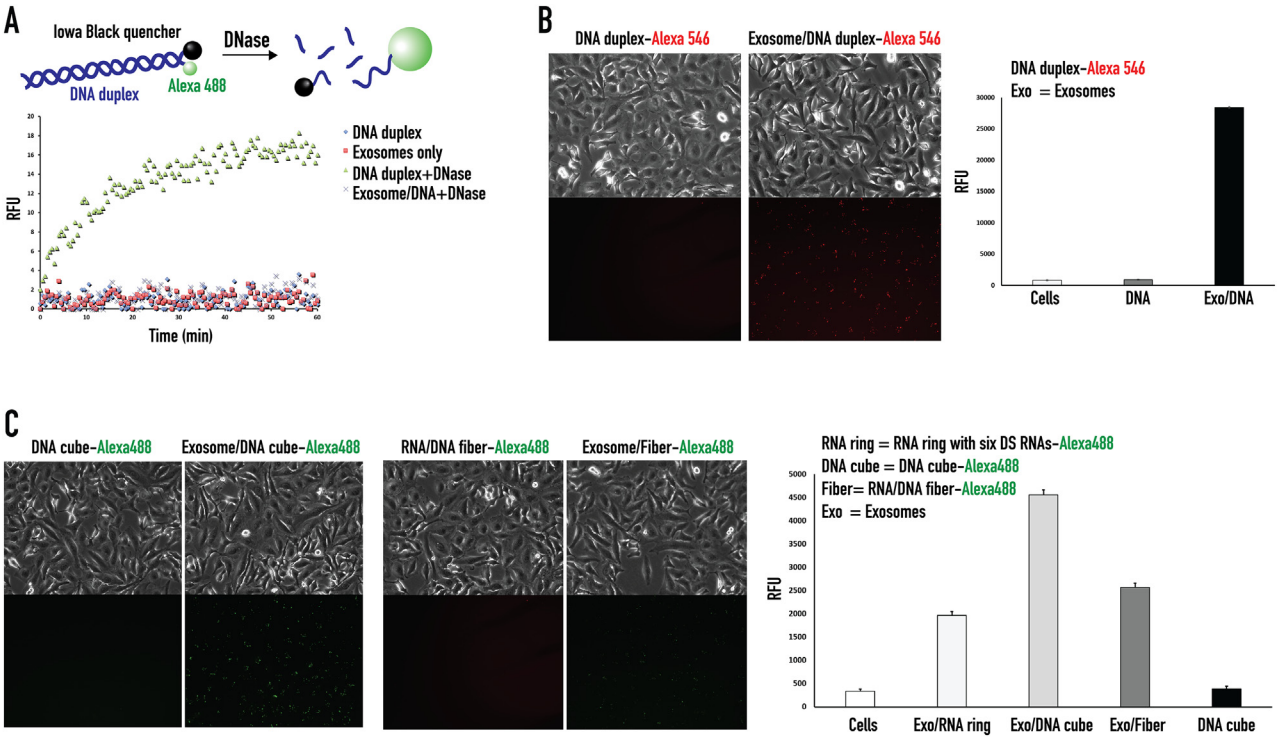

Figure 3. Exosomes protect nucleic acids cargo from enzymatic degradation and promote its cellular uptake. (**A**) Schematic diagram of nuclease digestion assay and assay results for DNA duplexes loaded exosomes after incubation with RQ1 DNAse. (**B**-**C**) Fluorescent microscope images of human breast cancer MDA-MB-231 show cell uptake of fluorescently labeled DNA duplexes (**B**) and NANPs (**C**) and the corresponding flow cytometry analysis.

downstream production of SEAP that can be detected and quantified using QUANTI-Blue™. THP1-Dual™ cells are engineered to express SEAP upon NF-kB stimulation, which can also be assessed by QUANTI-Blue™. In order to investigate the conditional activation of NF-kB decoys, Poly (I:C) (polyinosinic-polycytidylic acid, a synthetic analog of dsRNA) and Pam3CSK4 (a synthetic diacylated lipopeptide) were used to stimulate HEK-Blue™ hTLR3 and THP1-Dual™ cells, respectively. For the experiments with the HEK-Blue™ hTLR7 cells, R848 (resiquimod) was used as a positive control.

Results

Characterization of isolated exosomes

Extracellular vesicles are cell-derived membrane particles subdivided into microvesicles – ranging in size from 100 to 1000 nm – that are shed from the membrane and exosomes released by fusion of late endosomes with the cell membrane (30-150 nm size range) (Figure 1, *A*).[33–35] Although microvesicles and exosomes are structurally similar and overlap in size, their content and cell origins are different.[32] Exosomes secreted by MBA-MD-231(231) were isolated using ExoQuick-TC ULTRA. Prior to the addition of ExoQuick-TC reagent, centrifugation was used to remove cell debris and large particles, such as apoptotic bodies. The isolation method included two steps: (i) precipitation of exosomes with ExoQuick-TC and (ii) their purification with an affinity chromatography column, ULTRA. ExoQuick-TC ULTRA efficiently removes the major non-EV co-isolates, such as bovine albumin and bovine IgG, which usually are overrepresented in the tissue culture media.[54] Figure 1, *B* shows high amounts of albumin and IgG after precipitation step and demonstrates significant reduction of the co-isolated after the second step of ULTRA purification. Thus, the use of ExoQuick-TC ULTRA was essential to achieve the higher purity of isolated exosomes.

The ExoQuick-TC ULTRA isolation method yielded a particle concentration of 4.50E+11 ± 6.80E+10 particles/mL as measured by fluorescent NTA (fNTA) and 4.70E+11 ± 5.10E +10 particles/mL as measured by NTA (Figure 1, *C*). Since NTA measures any particle in solution, including protein aggregates and buffer precipitates, we specifically labeled exosomes with a membrane sensor dye and measured the concentration of intact vesicles using fNTA.[55,56] The mean diameter of the isolated exosomes was 103.5 ± 26.4 nm as fNTA and 123.1 ± 8.1 nm as measured by conventional NTA (Figure 1, *C*). A size distribution curve showed a classical distribution of exosomes ranging in size from 30 to 150 nm. Common exosomal markers Hsp70, ALIX, and tetraspanin, CD63, were identified (Figure 1, *B*). ALIX is an exosomal protein known for its involvement in the MVB biogenesis.[32] CD63 was enriched in exosomal membrane from different origins.[57,58] Hsp70 was released into the extracellular space *via* exosomes as a membrane- bound protein.[59] Calnexin is an integral protein of the endoplasmic reticulum (ER) and was used in as a cellular marker. Absence of calnexin marker in the exosome preparation indicated no cellular contamination was

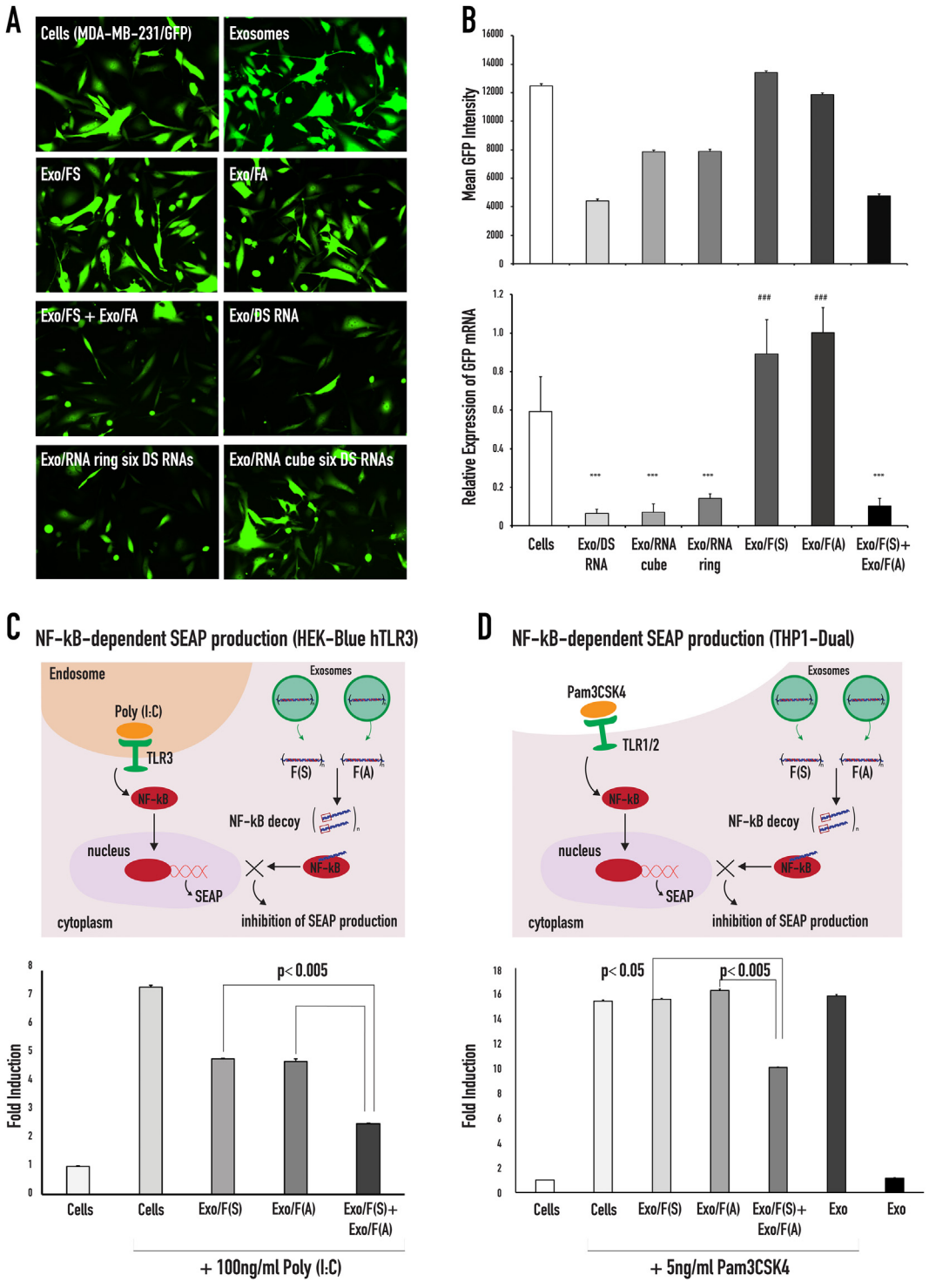

Figure 4. GFP silencing in MDA-MB-231/GFP cells treated with functionalized anti-GFP NANPs loaded into exosomes and inhibition of NF-kB function in HEK-Blue™ hTLR3 and THP1-Dual™ cells. (**A**) Fluorescent microscope images of MDA-MB-231-GFPs taken 72 h post treatment with exosomes and exosomes loaded with either NANPs. (**B**) Flow cytometry data of the mean GFP fluorescence and RT-qPCR analysis of the relative GFP expression of MDA-MB-231-GFP cells after 72 h of incubation with NANPs loaded exosomes. Statistical significance for the samples compared to the negative control is denoted by * (*** $P < 0.001$). Statistical significance of Exo/FS, Exo/FA compared to Exo/FS + Exo/FA is denoted by # (### $P < 0.001$). (**C**) Schematic demonstration of the TLR3 signaling that activates the NF-kB pathway and the assembly of the NF-kB decoys (upon re-association of the RNA/DNA fibers) that inhibits the nuclear translocation of the activated NF-kB. Poly (I:C) is used to activate the TLR3 ligand, the TLR3 signal resulted in the activation of NF-kB and subsequently NF-kB entered the nucleus, where it will bind to specific sequences of DNA to promote the downstream transcription and translation of secreted embryonic alkaline phosphatase (SEAP). The reporter cell line HEK-Blue™ hTLR3 was transfected with fibers and stimulated with Poly (I:C). The cells were incubated for 24 h, and the levels of NF-kB-dependent SEAP were measured in the supernatants. (**D**) Schematic demonstration of the TLR1/2 signaling that activates the NF-kB pathway that can be inhibited with the NF-kB decoys assembled upon re-association of RNA/DNA fibers (F(S) and F(A)).

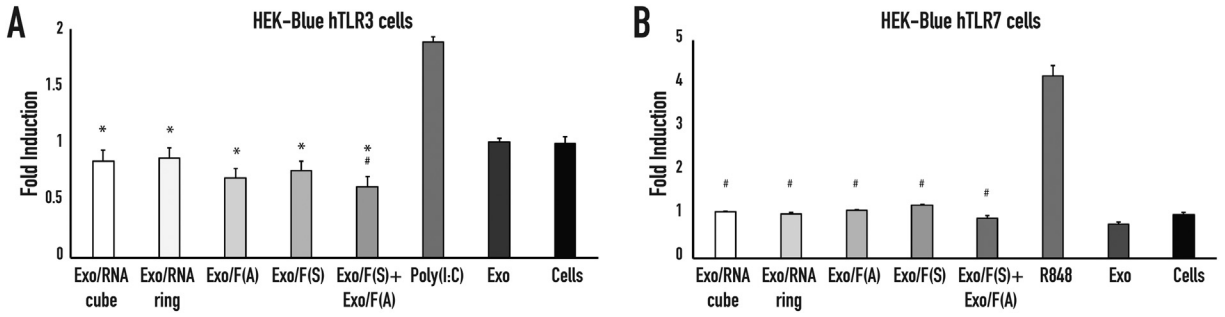

Figure 5. Relative levels of immunostimulation of exosomes loaded with NANPs. TLR stimulation is measured *via* SEAP secretion from (**A**) HEK-Blue™ hTLR3 and (**B**) HEK-Blue™ hTLR7 cells. In (**A**), statistical significance relevant to the cells is denoted by #, statistical significance relevant to poly I:C is denoted by * (# $P < 0.05$, * $P < 0.001$). In (**B**), statistical significance relevant to R848 is denoted by # ((# $P < 0.05$).

present. Transmission electron microscopy (TEM) images of isolated exosomes showed normal morphology without any distortion (Figure 1, *D*).[60] Altogether, we conclude that the isolated sample was enriched in exosomes based on our results.

Characterization of NANP loaded exosomes and nuclease protection assay

The NANPs used in this study have distinct, strategic designs that confer different compositions, connectivities, shapes, and sizes.[61] Both cube and ring RNA scaffolds are assembled from six individual RNAs; cubes are globular (3D), whereas rings are planar (2D). The hydrodynamic radii (based on DLS results) of cubes and rings functionalized with six anti-GFP DS RNAs were estimated to be ~12 and ~15 nm, respectively.[16,62] DNA/RNA fibers are linear (1D) and composed of both DNA and RNA strands. While RNA cubes and RNA/DNA fibers are assembled only *via* intermolecular Watson–Crick base pairing, assembly of RNA rings initially requires intramolecular Watson–Crick base pairing to further facilitate magnesium-dependent intermolecular kissing loop interactions.[63] Although each of these structures has distinct properties, all of them can be functionalized with DS RNAs that upon intracellular dicing release siRNAs designed to silence intended gene through sequence specific mRNA targeting. In addition, DNA/RNA fibers are functionalized with NF-kB decoys, inhibiting immune responses through the NF-kB pathway. All NANPs were analyzed by native-PAGE and AFM, as shown in Figure 2, *A*, to confirm the correct assembly.

To load NANPs into isolated exosomes, Exo-Fect siRNA/miRNA Transfection Kit was used. The Exo-Fect transfection reagent formed a complex with the NANPs and assisted with exosome insertion. Following the transfection, all samples were run through a clean-up column to remove excess Exo-Fect reagent, as well as free NANPs and their complexes. TEM images showed exosomes loaded with functionalized RNA rings, RNA cubes, and RNA/DNA fibers possessed morphology similar to free exosomes (Figure 1, *D* and Figure 2, *B*) with no associated structural changes. To verify the integrity of loaded exosomes, the presence of common exosomal markers (Hsp70, ALIX, and tetraspanin, CD63) was confirmed (Figure 2, *C*). Interestingly, NTA analysis indicated that exosomes originally with mean diameter of ~102-103 nm became larger by ~20-30 nm after loading with NANPs (Figure 2, *D*).

Next, the exosomes' ability to protect a loaded nucleic acid cargo from nuclease degradation were analyzed using a nuclease protection assay (Figure 3, *A*) developed from previous works.[19,22,64] As a model system, exosomes loaded with DNA duplexes labeled with Alexa 488 at the 5′-end and Iowa Black quencher at the complementary 3′-end were used. Due to the quencher's proximity to the fluorophore, the fluorescent signal from the DNA duplex was quenched. However, after RQ1 DNase treatment and subsequent DNA degradation, the fluorophore escaped from the quencher, leading to a progressively increasing fluorescent signal. At the same time, exosome-encapsulated DNA duplexes were protected from DNase digestion and yielded no changes in the fluorescent signal. Indeed, the miniscule increase in fluorescence proves that exosomes can effectively protect nucleic acid cargo from nuclease digestion. Free exosomes were used as controls to show that little to no signal appears in these samples. Results of this experiment suggest that exosomes were able to completely shield their nucleic acid cargos from degradation by enzymatic activity for at least 60 min.

Cellular uptake of exosomes loaded with NANPs

To confirm effective delivery of loaded NANPs, exosomes isolated from human breast cancer MDA-MB-231 (231) cells were loaded with either Alexa 488- or Alexa 546-labeled NANPs and added to 231 cells. Fluorescence microscopy images captured 24 h post-transfection validated the internalization of loaded exosomes into cells (Figure 3, *B-C*). Flow cytometry and microscopy results demonstrated that exosomes loaded with Alexa 546-labeled DNA duplex internalized into the cells and, with no exosomes present, no significant cellular uptake occurred (Figure 3, *B*). Interestingly, flow cytometry results show different transfection efficiencies of exosome-encapsulated Alexa 488-labeled NANPs, indicating that NANP polyplex shapes may potentially affect cellular uptake efficiency (Figure 3, *C*). Overall, data confirmed that NANP-loaded exosomes can be internalized by human cells with visible effects on transfection efficiency. Interestingly, we noticed that the uptake efficiency for the same number of NANP loaded exosomes is significantly lower for primary cell lines when compared to

cancer cells (supporting Figure S1). This may offer additional advantages for exosome mediated delivery of NANP, due to the potential reduction in undesired off-target effects in healthy tissues.

GFP gene silencing with functionalized NANP loaded exosomes

We achieved successful transfection of labeled NANPs into cells using exosomes as delivery vesicles. To confirm retention of the NANPs' intended function upon delivery, NANPs decorated with DS RNA against GFP[1,6,16,65] were used. Human breast cancer cells MDA-MB-231-GFP expressing GFP (231-GFP) were treated with a panel of exosomes loaded with anti-GFP-functionalized NANP polyplexes (Figure 4, *A-B*). Based on microscopy, flow cytometry, and RT-qPCR results, we found that 231-GFP cells treated with RNA ring- and RNA cube-loaded exosomes demonstrated a marked decrease in GFP expression. Exosomes loaded with sense (FS) or antisense (FA) RNA/DNA fibers did not change GFP expression individually; however, when both exosomes were added onto the same cell, there was a significant decrease in GFP expression. Therefore, fibers can re-associate and release DS RNAs only upon internalization with exosomes. Despite differences in shape, functional RNA cubes, RNA rings, and RNA/DNA fibers performed similarly in GFP silencing experiments (Figure 4, *A-B*), while no cytotoxicity was observed (supporting Figure S2).

Inhibition of NF-kB pathway

To further verify the intact dual functionality of DNA/RNA fibers that carry NF-kB response specificity and GFP silencing, we conducted a follow-up study using the reporter cell line HEK-Blue™ hTLR3. These cells are designed for the study of human TLR3 stimulation through assessment of NF-kB activation. The latter process induces production of secreted embryonic alkaline phosphatase (SEAP). Poly (I:C), a synthetic mimetic of viral dsRNA, can be used to trigger NF-kB activation and, ultimately, SEAP production (Figure 4, *C* and supporting Figure S3). In this experiment, cognate RNA/DNA fibers (FS and FA) were separately pre-loaded into exosomes which were then mixed together for co-delivery (see FS/Exo + FA/Exo). Individual FS- and FA-loaded exosomes were used as controls (see FS/Exo and FA/Exo). On the same day that the complexes were added to the HEK-Blue™ hTLR3 cells, the cells were challenged with Poly (I:C). Supernatants were then collected and analyzed for presence of secreted alkaline phosphatase (SEAP), which can be easily detected and quantified using QUANTI-Blue™ reagent. Cells treated with poly (I:C) produced significant SEAP signal, and when FS and FA were delivered separately, no inhibition in SEAP production was observed. However, co-delivered of FS and FA significantly reduced SEAP synthesis. To show the generality, another reporter cell line – THP1-Dual™ – that also expressed SEAP under the NF-kB promoter was tested (Figure 4, *D*). To induce the activation of the NF-kB pathway, THP1-Dual™ cells were challenged with a TLR agonist (PAM3CSK4). On the same day, exosomes loaded with fibers were added to PAM3CSK4 treated cells and the supernatants were collected and analyzed for the presence of SEAP. The cells treated with Pam3CSK4 induced significant SEAP production, and when FS and FA were delivered separately, no inhibition of SEAP was observed. However, co-delivered FS and FA reduced SEAP production. These results were consistent with Lipofectamine 2000's actions as a transfection reagent, as described previously.[65] When the cells were treated with Poly (I:C) for 24 h prior to addition of RNA/DNA fibers and then incubated for an additional 24 h, the extent of SEAP inhibition was decreased (supporting Figure S1). All of these results support intracellular release of NANPs without any loss of their intended function.

Immunostimulation by exosome loaded NANPs

Another nucleic acid-specific TLR was investigated using HEK-Blue™ hTLR7 cells. Both HEK-Blue™ hTLR 3 and 7 cells were obtained by co-transfection of the hTLR gene into HEK293 cells and engineered to express a single Toll-like receptor. Stimulation of TLR7 with R848, an imidazoquinoline and agonist of TLR7, led to production of SEAP whose levels can be determined using HEK-Blue™ detection reagent in real time. Here, we used these cells to evaluate the potential immunostimulation by the NANP/exosome complexes (Figure 5). Both TLR3 and TLR7 are responsible for RNA detection, while TLR3 activated by dsRNA and TLR7 detects ssRNA.[66] Our data confirmed stimulation from both TLR3 and TLR7 cells to be negligible.

Discussion

Here, we demonstrated exosome-mediated delivery of different NANPs exhibiting various shapes and structures and investigated their intracellular uptake, post-delivery gene silencing efficiency, and immunostimulation potential. Exosome loading with NANPs of various sizes can be challenging and numerous methods have been developed to efficiently facilitate the transfection. One technique is chemical transfection, which shows promising results for direct cargo loading. Exo-Fect™ siRNA/miRNA transfection kit (System Biosciences, Palo Alto, CA, USA) has shown positive results for nucleic acid transfection into exosomes (unpublished results). In order to load the cube, ring, and fiber NANPs into exosomes, Exo-Fect reagent forms a complex with the nucleic acids. We showed that exosomes remain intact post packaging and retain the common exosomal marker such as CD63. Interestingly, we noticed that the exosomes become slightly bigger upon NANPs loading. We demonstrated that NANPs loaded into exosomes with intact shape reassumed their original functionalities upon delivery (Figure 6) and effectively silenced GFP in the cells that constitutively express GFP. In our earlier studies using HEK 293 cells that overexpress human TLR7 and the SEAP genes, we showed that the RNA cubes delivered by L2K and PgP induced SEAP production when placed under the control of an NF-kB and AP-1-inducible promoter.[61,67] In contrast, even for the RNA cubes (known for displaying the greatest immunostimulatory properties) we observed negligible immune response after using exosomes to deliver these structures. Our data suggest that

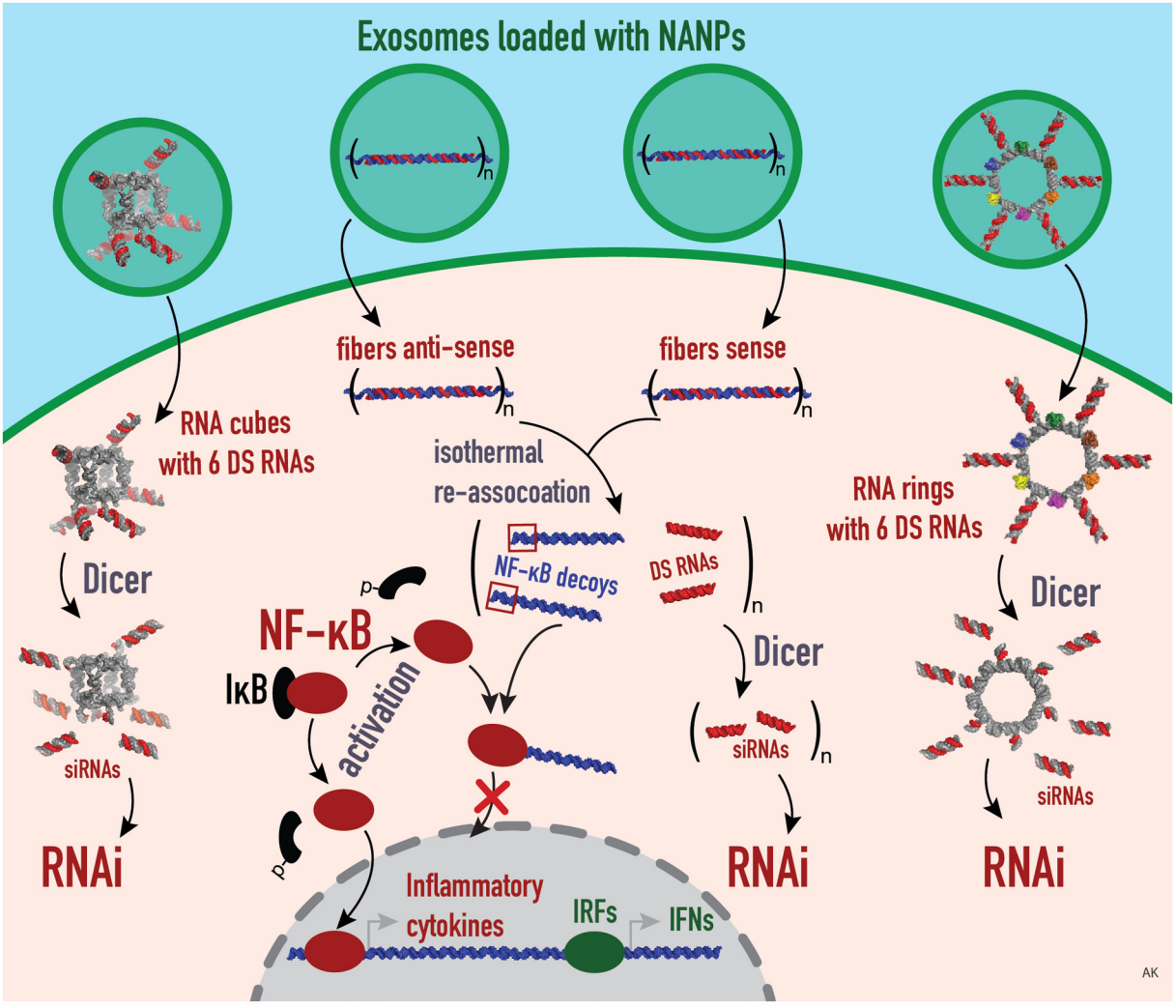

Figure 6. Schematic summary of the proposed mechanism of exosome-mediated delivery of different functionalized NANPs. Exosomes are loaded with NANPs, such as RNA cubes and RNA rings, that are functionalized with 6 DSRNAs, and fiber antisense and fiber sense that carry *n* numbers of DS RNAs and NF-kB decoys. Those NANPs are delivered by exosomes and released inside the target cells. In the cytosol, the DS RNAs will be further diced by Dicer to result in the generation of siRNAs, by which the RNAi pathway is activated. Meanwhile, the NF-kB decoys are released from the fibers, which in turn bind to NF-kB in order to prevent its nuclear translocation, thus inhibiting the downstream production of IRF and IFNs.

exosome-mediated NANP delivery can potentially "stealth-coat" exosome contents from certain pattern recognition receptors, but further studies are required. In summary, this work may pave the way towards the efficient and safe application of NANPs in personalized medicine by implementing patient-derived exosomes as a novel and promising therapeutic platform.

Appendix A. Supplementary data

Supplementary data to this article can be found online at https://doi.org/10.1016/j.nano.2020.102285.

References

1. Afonin KA, Viard M, Koyfman AY, Martins AN, Kasprzak WK, Panigaj M, et al. Multifunctional RNA nanoparticles. *Nano Lett* 2014;**14**(10):5662-71.
2. Afonin Kirill A, Lindsay B, Shapiro Bruce A. Engineered RNA nanodesigns for applications in RNA nanotechnology. *DNA and RNA Nanotechnology* 2013;**1**:1-15.
3. Grabow WW, Jaeger L. RNA self-assembly and RNA nanotechnology. *Acc Chem Res* 2014;**47**(6):1871-80.
4. Lee H, Lytton-Jean AKR, Chen Y, Love KT, Park AI, Karagiannis ED, et al. Molecularly self-assembled nucleic acid nanoparticles for targeted in vivo siRNA delivery. *Nat Nanotechnol* 2012;**7**(6):389-93.
5. Afonin KA, Bindewald E, Yaghoubian AJ, Voss N, Jacovetty E, Shapiro BA, et al. In vitro assembly of cubic RNA-based scaffolds designed in silico. *Nat Nanotechnol* 2010;**5**(9):676-82.
6. Rackley L, Stewart JM, Salotti J, Krokhotin A, Shah A, Halman JR, et al. RNA fibers as optimized nanoscaffolds for siRNA coordination and reduced immunological recognition. 2018;**28**(48):1805959.
7. Bui MN, Johnson MB, Viard M, Satterwhite E, Martins AN, Li Z, et al. Versatile RNA tetra-U helix linking motif as a toolkit for nucleic acid nanotechnology. 2017;**13**(3):1137-46.
8. Rose SD, Kim DH, Amarzguioui M, Heidel JD, Collingwood MA, Davis ME, et al. Functional polarity is introduced by Dicer processing of short substrate RNAs. *Nucleic Acids Res* 2005;**33**(13):4140-56.

9. Afonin KA, Viard M, Kagiampakis I, Case CL, Dobrovolskaia MA, Hofmann J, et al. Triggering of RNA interference with RNA-RNA, RNA-DNA, and DNA-RNA nanoparticles. *ACS Nano* 2015;**9**(1):251-9.
10. Chandler M, Panigaj M, Rolband LA, Afonin KA. Challenges to optimizing RNA nanostructures for large scale production and controlled therapeutic properties. *Nanomedicine (Lond)* 2020;**15**(13):1331-40.
11. Panigaj M, Johnson MB, Ke W, McMillan J, Goncharova EA, Chandler M, et al. Aptamers as modular components of therapeutic nucleic acid nanotechnology. *ACS Nano* 2019;**13**(11):12301-21.
12. Afonin KA, Dobrovolskaia MA, Church G, Bathe M. Opportunities, barriers, and a strategy for overcoming translational challenges to therapeutic nucleic acid nanotechnology. *ACS Nano* 2020;**14**(8):9221-7.
13. Afonin KA, Viard M, Martins AN, Lockett SJ, Maciag AE, Freed EO, et al. Activation of different split functionalities on re-association of RNA-DNA hybrids. *Nat Nanotechnol* 2013;**8**(4):296-304.
14. Halman JR, Satterwhite E, Roark B, Chandler M, Viard M, Ivanina A, et al. Functionally-interdependent shape-switching nanoparticles with controllable properties. *Nucleic Acids Res* 2017;**45**(4):2210-20.
15. Chandler M, Afonin KA. Smart-responsive nucleic acid nanoparticles (NANPs) with the potential to modulate immune behavior. *Nanomaterials (Basel)* 2019;**9**(4).
16. Afonin KA, Desai R, Viard M, Kireeva ML, Bindewald E, Case CL, et al. Co-transcriptional production of RNA-DNA hybrids for simultaneous release of multiple split functionalities. *Nucleic Acids Res* 2014;**42**(3):2085-97.
17. Ke W, Hong E, Saito RF, Rangel MC, Wang J, Viard M, et al. RNA-DNA fibers and polygons with controlled immunorecognition activate RNAi, FRET and transcriptional regulation of NF-kappaB in human cells. *Nucleic Acids Res* 2019;**47**(3):1350-61.
18. Porciani D, Tedeschi L, Marchetti L, Citti L, Piazza V, Beltram F, et al. Aptamer-mediated codelivery of doxorubicin and NF-kappaB decoy enhances chemosensitivity of pancreatic tumor cells. *Mol Ther Nucleic Acids* 2015;**4**e235.
19. Kim KH, Lee ES, Cha SH, Park JH, Park JS, Chang YC, et al. Transcriptional regulation of NF-kappaB by ring type decoy oligodeoxynucleotide in an animal model of nephropathy. *Exp Mol Pathol* 2009;**86**(2):114-20.
20. Griesenbach U, Scheid P, Hillery E, de Martin R, Huang L, Geddes DM, et al. Anti-inflammatory gene therapy directed at the airway epithelium. *Gene Ther* 2000;**7**(4):306-13.
21. Parlea L, Puri A, Kasprzak W, Bindewald E, Zakrevsky P, Satterwhite E, et al. Cellular delivery of RNA nanoparticles. *ACS Comb Sci* 2016;**18**(9):527-47.
22. Halman JR, Kim KT, Gwak SJ, Pace R, Johnson MB, Chandler MR, et al. A cationic amphiphilic co-polymer as a carrier of nucleic acid nanoparticles (Nanps) for controlled gene silencing, immunostimulation, and biodistribution. *Nanomedicine* 2020;**23**:102094.
23. Gupta K, Mattingly SJ, Knipp RJ, Afonin KA, Viard M, Bergman JT, et al. Oxime ether lipids containing hydroxylated head groups are more superior siRNA delivery agents than their nonhydroxylated counterparts. *Nanomedicine (Lond)* 2015;**10**(18):2805-18.
24. Gupta K, Afonin KA, Viard M, Herrero V, Kasprzak W, Kagiampakis I, et al. Bolaamphiphiles as carriers for siRNA delivery: from chemical syntheses to practical applications. *J Control Release* 2015;**213**:142-51.
25. Cruz-Acuna M, Halman JR, Afonin KA, Dobson J, Rinaldi C. Magnetic nanoparticles loaded with functional RNA nanoparticles. *Nanoscale* 2018;**10**(37):17761-70.
26. Tiwari G, Tiwari R, Sriwastawa B, Bhati L, Pandey S, Pandey P, et al. Drug delivery systems: an updated review. *Int J Pharm Investig* 2012;**2**(1):2-11.
27. Makhmalzade BS, Chavoshy F. Polymeric micelles as cutaneous drug delivery system in normal skin and dermatological disorders. *J Adv Pharm Technol Res* 2018;**9**(1):2-8.
28. Bhaskar S, Tian F, Stoeger T, Kreyling W, de la Fuente JM, Grazú V, et al. Multifunctional Nanocarriers for diagnostics, drug delivery and targeted treatment across blood-brain barrier: perspectives on tracking and neuroimaging. *Part Fibre Toxicol* 2010;**7**:3.
29. Yan JF, Zhu JH, Cui MF, Zhang J, Ma F, Su YP, et al. Multifunctional mineral hydrogels: potential in artificially intelligent skins and drug delivery. *Acs Omega* 2019;**4**(21):19145-52.
30. Czapar AE, Steinmetz NF. Plant viruses and bacteriophages for drug delivery in medicine and biotechnology. *Curr Opin Chem Biol* 2017;**38**:108-16.
31. Das CK, Jena BC, Banerjee I, Das S, Parekh A, Bhutia SK, et al. Exosome as a novel shuttle for delivery of therapeutics across biological barriers. *Mol Pharm* 2019;**16**(1):24-40.
32. Raposo G, Stoorvogel W. Extracellular vesicles: exosomes, microvesicles, and friends. *J Cell Biol* 2013;**200**(4):373-83.
33. Lo Cicero A, Stahl PD, Raposo G. Extracellular vesicles shuffling intercellular messages: for good or for bad. *Curr Opin Cell Biol* 2015;**35**:69-77.
34. Abels ER, Breakefield XO. Introduction to extracellular vesicles: biogenesis, RNA cargo selection, content, release, and uptake. *Cell Mol Neurobiol* 2016;**36**(3):301-12.
35. Simons M, Raposo G. Exosomes—vesicular carriers for intercellular communication. *Curr Opin Cell Biol* 2009;**21**(4):575-81.
36. Ha D, Yang N, Nadithe V. Exosomes as therapeutic drug carriers and delivery vehicles across biological membranes: current perspectives and future challenges. *Acta Pharmaceutica Sinica B* 2016;**6**(4):287-96.
37. van Niel G, Porto-Carreiro I, Simoes S, Raposo G. Exosomes: a common pathway for a specialized function. *J Biochem* 2006;**140**(1):13-21.
38. Zhang Y, Liu Y, Liu H, Tang WH. Exosomes: biogenesis, biologic function and clinical potential. *Cell Biosci* 2019;**9**(1):19.
39. Tian T, Wang Y, Wang H, Zhu Z, Xiao Z. Visualizing of the cellular uptake and intracellular trafficking of exosomes by live-cell microscopy. *J Cell Biochem* 2010;**111**(2):488-96.
40. Saeedi S, Israel S, Nagy C, Turecki G. The emerging role of exosomes in mental disorders. *Transl Psychiatry* 2019;**9**(1):1-11.
41. Parolini I, Federici C, Raggi C, Lugini L, Palleschi S, De Milito A, et al. Microenvironmental pH is a key factor for exosome traffic in tumor cells. *J Biol Chem* 2009;**284**(49):34211-22.
42. Marcus ME, Leonard JN. FedExosomes: engineering therapeutic biological nanoparticles that truly deliver. *Pharmaceuticals (Basel)* 2013;**6**(5):659-80.
43. Valadi H, Ekström K, Bossios A, Sjöstrand M, Lee JJ, Lötvall JO. Exosome-mediated transfer of mRNAs and microRNAs is a novel mechanism of genetic exchange between cells. *Nat Cell Biol* 2007;**9**(6):654-9.
44. Aqil F, Munagala R, Jeyabalan J, Agrawal AK, Kyakulaga AH, Wilcher SA, et al. Milk exosomes — natural nanoparticles for siRNA delivery. *Cancer Lett* 2019;**449**:186-95.
45. Banizs AB, Huang T, Dryden K, Berr SS, Stone JR, Nakamoto RK, et al. In vitro evaluation of endothelial exosomes as carriers for small interfering ribonucleic acid delivery. *Int J Nanomedicine* 2014;**9**:4223-30.
46. Shtam TA, Kovalev RA, Varfolomeeva EY, Makarov EM, Kil YV, Filatov MV. Exosomes are natural carriers of exogenous siRNA to human cells in vitro. *Cell Commun Signal* 2013;**11**:10.
47. Yang R, Yan X, Zhang S, Guo HJTJoU. MP88-16 targeted exosome-mediated delivery of survivin sirna for the treatment of bladder cancer. 2017.
48. Kamerkar S, LeBleu VS, Sugimoto H, Yang S, Ruivo CF, Melo SA, et al. Exosomes facilitate therapeutic targeting of oncogenic KRAS in pancreatic cancer. *Nature* 2017;**546**(7659):498-503.
49. Barile L, Vassalli G. Exosomes: therapy delivery tools and biomarkers of diseases. *Pharmacol Ther* 2017;**174**:63-78.
50. Ha D, Yang N, VJAPSB Nadithe. Exosomes as therapeutic drug carriers and delivery vehicles across biological membranes: current perspectives and future challenges. 2016;**6**(4):287-96.
51. Kibria G, Ramos EK, Wan Y, Gius DR, Liu H. Exosomes as a drug delivery system in cancer therapy: potential and challenges. *Mol Pharm* 2018;**15**(9):3625-33.

52. Murphy DE, de Jong OG, Brouwer M, Wood MJ, Lavieu G, Schiffelers RM, et al. Extracellular vesicle-based therapeutics: natural versus engineered targeting and trafficking. *Exp Mol Med* 2019;**51**(3):1-12.
53. Zhang Y, Liu Y, Liu H, Tang WHJC. Exosomes: biogenesis, biologic function and clinical potential. 2019;9(1):19.
54. Thery C, Witwer KW, Aikawa E, Alcaraz MJ, Anderson JD, Andriantsitohaina R, et al. Minimal information for studies of extracellular vesicles 2018 (MISEV2018): a position statement of the International Society for Extracellular Vesicles and update of the MISEV2014 guidelines. *J Extracell Vesicles* 2018;**7**(1):1535750.
55. Andrew Malloy DG, Hole Patrick, Carr Bob. Counting and sizing of viral vector particles and aggregates by nanoparticle tracking analysis (NTA). *MUSCULO-SKELETAL GENE & CELL THERAPY IIIIIII* 2010;**18**(S223).
56. McNicholas K, Li JY, Michael MZ, Gleadle JM. Albuminuria is not associated with elevated urinary vesicle concentration but can confound nanoparticle tracking analysis. *Nephrology (Carlton)* 2017;**22**(11):854-63.
57. Escola JM, Kleijmeer MJ, Stoorvogel W, Griffith JM, Yoshie O, Geuze HJ. Selective enrichment of tetraspan proteins on the internal vesicles of multivesicular endosomes and on exosomes secreted by human B-lymphocytes. *J Biol Chem* 1998;**273**(32):20121-7.
58. Zoller M. Tetraspanins: push and pull in suppressing and promoting metastasis. *Nat Rev Cancer* 2009;**9**(1):40-55.
59. Chanteloup G, Cordonnier M, Isambert N, Bertaut A, Marcion G, Garrido C, et al. Membrane-bound exosomal HSP70 as a biomarker for detection and monitoring of malignant solid tumours: a pilot study. *Pilot Feasibility Stud* 2020;**6**:35.
60. Wu Y, Deng W, Klinke 2nd DJ. Exosomes: improved methods to characterize their morphology, RNA content, and surface protein biomarkers. *Analyst* 2015;**140**(19):6631-42.
61. Hong EP, Halman JR, Shah AB, Khisamutdinov EF, Dobrovolskaia MA, Afonin KA. Structure and composition define immunorecognition of nucleic acid nanoparticles. *Nano Lett* 2018;**18**(7):4309-21.
62. Afonin KA, Grabow WW, Walker FM, Bindewald E, Dobrovolskaia MA, Shapiro BA, et al. Design and self-assembly of siRNA-functionalized RNA nanoparticles for use in automated nanomedicine. *Nat Protoc* 2011;**6**(12):2022-34.
63. Grabow WW, Zakrevsky P, Afonin KA, Chworos A, Shapiro BA, Jaeger L. Self-assembling RNA nanorings based on RNAI/II inverse kissing complexes. *Nano Lett* 2011;**11**(2):878-87.
64. Kim T, Viard M, Afonin KA, Gupta K, Popov M, Salotti J, et al. Characterization of cationic bolaamphiphile vesicles for siRNA delivery into tumors and brain. *Mol Ther Nucleic Acids* 2020;**20**:359-72.
65. Ke W, Hong E, Saito RF, Rangel MC, Wang J, Viard M, et al. RNA–DNA fibers and polygons with controlled immunorecognition activate RNAi, FRET and transcriptional regulation of NF-κB in human cells. *Nucleic Acids Res* 2018;**47**(3):1350-61.
66. Ohto U, Shimizu T. Structural aspects of nucleic acid-sensing Toll-like receptors. *Biophys Rev* 2016;**8**(1):33-43.
67. Halman JR, Kim K-T, Gwak S-J, Pace R, Johnson MB, Chandler MR, et al. A cationic amphiphilic co-polymer as a carrier of nucleic acid nanoparticles (Nanps) for controlled gene silencing, immunostimulation, and biodistribution. Nanomedicine: Nanotechnology. *Biology and Medicine* 2020;**23**:102094.